NRIAG Journal of Astronomy and Geophysics (2016) 5, 160–172

National Research Institute of Astronomy and Geophysics

NRIAG Journal of Astronomy and Geophysics

www.elsevier.com/locate/nrjag

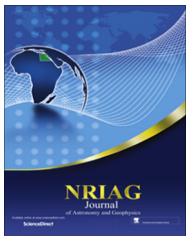

Natural radioactivity and radiation hazard assessment of phosphate mining, Quseir-Safaga area, Central Eastern Desert, Egypt

Ibrahim Gaafar [a,*], **Amal El-Shershaby** [b], **Ibrahim Zeidan** [a], **Lina Sayed El-Ahll** [b]

[a] *Nuclear Materials Authority, Cairo, Egypt*
[b] *Faculty of Women for Arts, Science and Education, Ain Shams University, Cairo, Egypt*

Received 20 January 2016; revised 8 February 2016; accepted 8 February 2016
Available online 23 February 2016

KEYWORDS

Carborne spectrometric survey;
Uranium;
Phosphate;
Dose rate

Abstract Quseir-Safaga area, Central Eastern Desert, Egypt, includes Duwi Formation, which contains uranium-bearing phosphate beds. The present work used the integrated carborne γ-ray spectrometric data, X-ray analysis and HPGe γ-ray spectrometer data to investigate the radioactive zones at this area. Carborne γ-ray spectrometric survey revealed an increase of equivalent uranium, up to 182 ppm. Maps were drawn to show the results of the three radioelements K, eU, eTh and the eU/eTh ratio. The eU and (eU/eTh) maps reveal that there are twelve important anomalies, associated mainly with phosphate mines. The Hamrawein mines at the northwestern part in the study area seem to represent the highest U-anomalies.

Twelve phosphate samples were collected from the determined twelve anomalies. They were analyzed with HPGe detector gamma-ray spectrometer. It was found that the results of radioelement concentrations by carborne survey agree well with that obtained by HPGe. Both of them show that phosphate mines effectively contribute to eU anomalies, occurring in the study area. Meanwhile, ^{40}K, ^{238}U and ^{232}Th concentrations in phosphate samples range from 91 to 169, 864 to 3104 and 28.4 to 106 Bq/kg respectively. The highest concentration of ^{238}U (3104 Bq/kg) occurs in the north of the studied area, close to Hamrawein city. The average concentration of ^{238}U in the analyzed samples is 1766 Bq/kg, which is 53 times higher than the worldwide average value reaching 33 Bq/kg. The highest ^{232}Th concentration value reaching 106 Bq/kg is 2.4 times higher than the worldwide value attaining 45 Bq/kg. The absorbed dose rate for the phosphate samples shows the highest value reaching 1468 nGy/h. This is more than 25 times the worldwide average value 58 nGy/h. The annual effective absorbed dose is also high and reached 1.8 mSv/y, which is about twice higher than the permitted value for public exposure of 1.0 mSv/y. The maximum external hazardous index value of 9.2 is more than nine times the unity permitted in ICRP, 2000.

* Corresponding author.
Peer review under responsibility of National Research Institute of Astronomy and Geophysics.

http://dx.doi.org/10.1016/j.nrjag.2016.02.002

1. Introduction

Radioactivity is the emission of alpha (α) and beta (β) particles as well as gamma (γ) radiation from the unstable isotopes. Most minerals, that contain potassium, uranium and thorium, are radioactive. Long-live radioactive elements such as uranium (^{238}U), thorium (^{232}Th) and potassium (^{40}K) and any of their decay products, such as radium and radon are examples of naturally occurring radioactive materials (NORM). Study of natural radioactivity is usually done in order to gain information about the present levels of harmful pollutants discharged to the environment itself or in the living creatures (UNSCEAR, 2000). Several studies were performed in different countries to determine the radionuclide concentrations in different food samples and dose assessments from consumption of foodstuff by the population (Shanthi et al., 2010; James et al., 2013).

Phosphates are used extensively, as a source of phosphorous for fertilizers and for manufacturing phosphoric acid and gypsum. Phosphate ores typically contain about 1500 Bq/kg of uranium and radium, although some phosphates contain up to 20,000 Bq/kg of U_3O_8 (Paschoa and Godoy, 2002). In general, phosphate ores of sedimentary origin have higher concentrations of radionuclides of the uranium family. In 90% of cases, the ore is treated with sulfuric acid. The fertilizers become somewhat enriched in uranium (up to 150% relative to the ore), while 80% of the ^{226}Ra, 30% of ^{232}Th and 5% of uranium are left in phosphogypsum (UNSCEAR, 2008).

The processing of phosphates may generate gaseous and particulate emissions that contain ^{238}U and ^{226}Ra, when discharged to the environment, lead to expose the population to radiation hazards. Local dump sites for phosphogypsum are usually not protected from rainfall and become hydraulically connected to surface water and shallow aquifers (Vandenhove, 2000). The use of phosphate fertilizers in agriculture and of gypsum in building materials is a further source of possible exposure to the public (Paschoa and Godoy, 2002). Elevated radon exposure to the public can further be expected in sites being developed for housing (Vandenhove, 2000).

2. Geologic setting

Quseir-Safaga area is located in the Central Eastern Desert of Egypt, between latitudes 25°58′N and 26°22′N and longitudes 34°03′E and 34°22′E (Fig. 1).

The phosphate ore deposits of Egypt represent a part of the Mediterranean Phosphate Province, which extends from Morocco to Turkey. They consist of strata deposited, on the shallow Tethyan seafloor, during Late Cretaceous and Early Tertiary times. Over a zone at central eastern desert of Egypt, between 24° and 27°N latitudes, these strata are nearly horizontal, but in the Red Sea area folding and block faulting have resulted in tilting of the mineable beds. The phosphate beds were estimated to contain in excess of 3 billion tons of ore (Notholt, 1985). In the region of the Eastern Desert of Egypt (Red Sea Coast), the phosphate-bearing strata are known as Duwi Formation, in the Nile Valley region as the Sibaiya

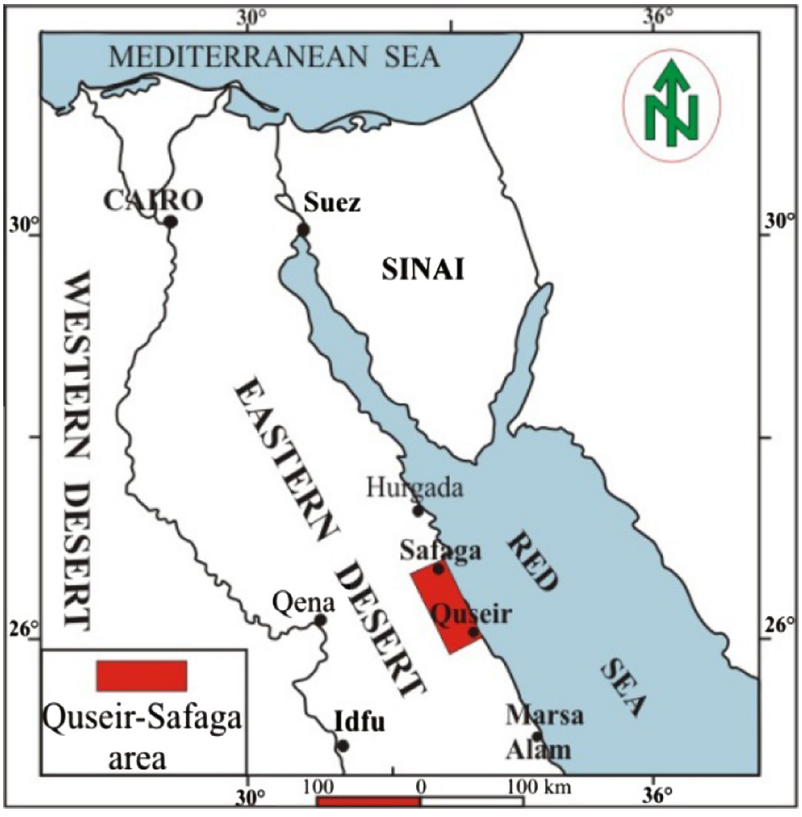

Figure 1 Location map of Quseir-Safaga area, Central Eastern Desert, Egypt.

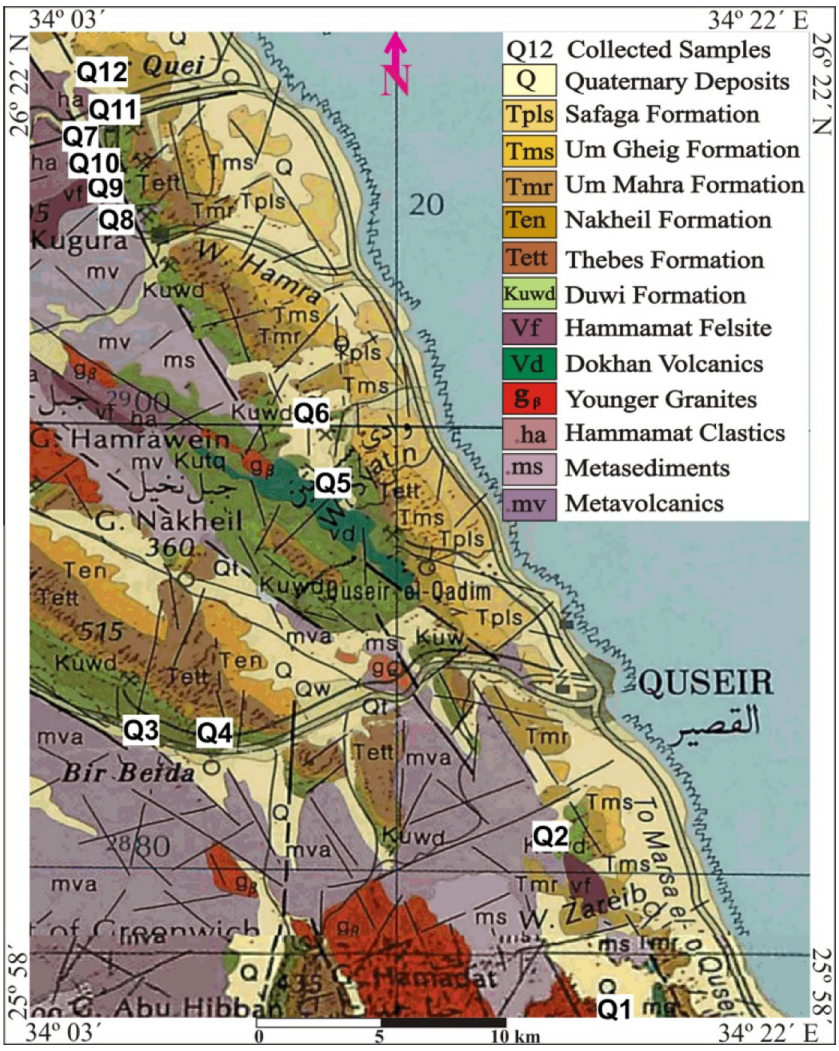

Figure 2 Geologic map of Quseir-Safaga area, Central Eastern Desert, Egypt (after CONOCO, 1987).

Phosphate Formation and in Western Desert as Phosphate Formation (Awad and Ghobrial, 1966). These beds rest with seeming conformity on the Nubia sandstones and are overlain by deeper-water marls and chalks of the Dakhla Formation (Fig. 2).

The mineralogy of the Egyptian phosphate deposits was studied by many investigators (Dabous, 1981; Sharafeldin, 1999). The major phosphate mineral is carbonate-fluorapatite. The non-phosphatic minerals are represented by dolomite, calcite, quartz, pyrite, goethite, gypsum, smectite, and kaolinite. The clay minerals, associated with Egyptian phosphates, occur mainly as a matrix or a filling of the intergranular pores. Some clay minerals are also present as parts of the phosphatic pellets, or as fillings of the cavity-like microstructures in the bone and teeth fragments. Smectite is the dominant clay mineral, followed by kaolinite, whereas illite and palygorskite are present in trace concentrations (Sharafeldin, 1999). This mode of occurrence was also reported in the Miocene phosphates of Florida (Compton, 1997), the Cretaceous phosphates of Morocco (Prevot, 1990), and the Jordanian Cretaceous phosphates (Khoury et al., 1988). The iron minerals: goethite, hematite, and pyrite were found as coatings on the outer surfaces of phosphate pellets and parts of the cementing material (Dabous, 1981; Sharafeldin, 1999).

3. Carborne gamma-ray spectrometric surveys

The ability of gamma-ray spectrometry to map potassium, uranium, and thorium enrichment or depletion provides powerful exploration guidance in a wide variety of geological settings. Carborne gamma-ray spectrometry was used for source search (Ulvsand et al., 2002), contamination surveying and mapping (Karlsson et al., 2000; Sanderson et al., 2003) and prospecting (Grasty and Cox, 1997). Variations in the radioactivity of rocks may be useful for geological mapping (Aissa and Jubeli, 1997; Gaafar et al., 2016), for acquiring information on the distribution of radiation exposure rates (Raghuwanshi, 1992; Gaafar et al., 2014), and for environmental monitoring (Tauchid and Jubeli, 1991; Gaafar et al., 2012). Total gamma radioactivity can be used by health physicists for acquiring information on the distribution of radiation exposure rates (Raghuwanshi, 1992). Besides, a carborne radiometric system can be effectively used for an emergency

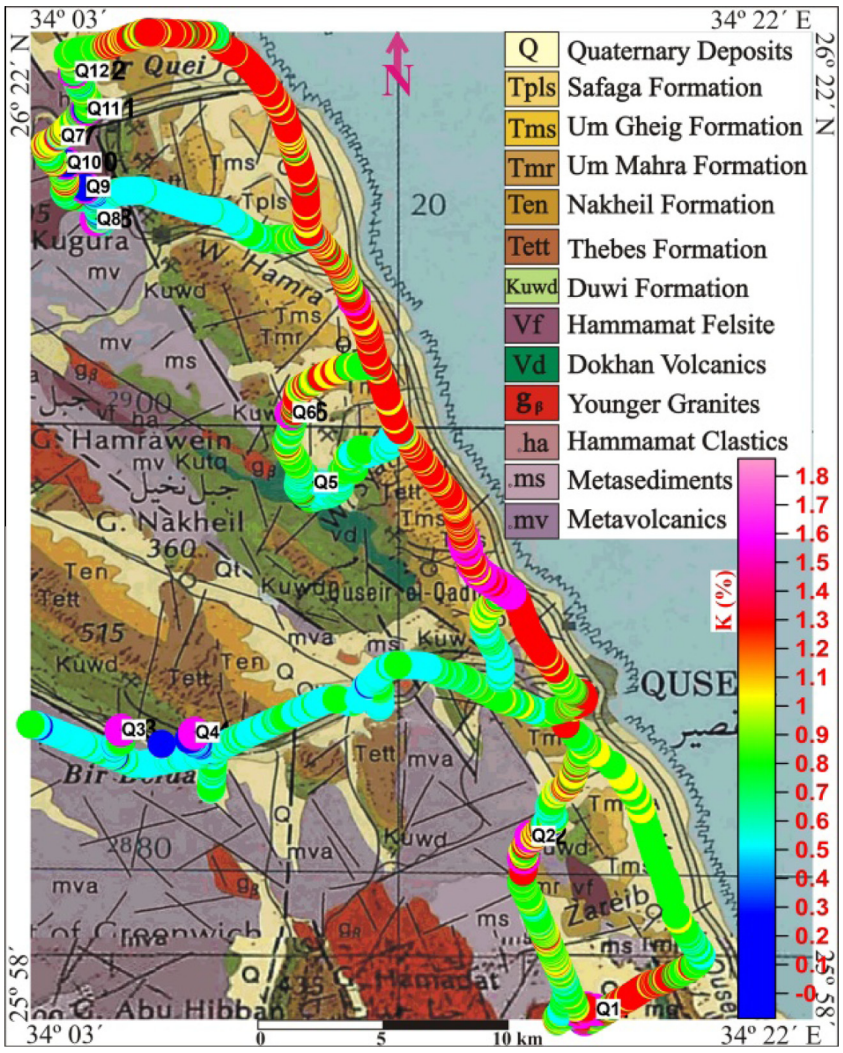

Figure 3 K (%) image distribution map of Quseir-Safaga area, Central Eastern Desert, Egypt.

response action due to radioactive incident or contamination (Tauchid and Jubeli, 1991).

3.1. Spectrometric survey

The carborne gamma-ray spectrometric system that used in the present survey is composed of a GR-320 portable multichannel gamma-ray spectrometer and has typically a 4 l NaI(Tl) scintillation detector. The position for each measurement point was determined by a GPS instrument and recorded with the spectrometric data. The complete system, loaded in a field car, was used to radioactive mineral and environmental exploration after calibration on NMA 4 standard calibration pads. A lot of collected spectrometric data confirm that the system is stable and works reliably, and is a fast and advanced approach for radioactive mineral γ-ray spectrometric exploration. It can be used not only to determine the contents of natural radioactive elements in environment, but also to monitor nuclear pollution and emergency treatment in nuclear accidents significantly.

Gamma-ray spectrometry provides a direct measurement of the surface distribution of naturally occurring radioelements (K, U, and Th). Potassium is a major constituent of most rocks, while uranium and thorium are present in trace amounts, as mobile and immobile elements, respectively. As the concentrations of these radioelements vary between different rock types, the measured radioelement distribution can be reliably used to map and distinguish different lithologies (IAEA, 2010). The concentrations of K, eU and eTh and eU/eTh ratio are illustrated along the image maps as shown in Figs. 3–6. There are twelve eU anomalies distributed along the car traverses, from south to north direction, having the values of: 66, 35, 57, 98, 80, 77, 97, 143, 182, 152, 116 and 85 ppm respectively (Fig. 4 and Table 1). The eU/eTh ratio shows strong positive correlation with eU, suggesting uranium mobilization in the phosphate that located in the northwest part of the studied area. The strong positive correlation between eU/eTh ratio and eU and the negative correlation between eU/eTh ratio and eTh coincide with phosphate mines (Figs. 4–6). The prominent high eU/eTh ratios are associated with phosphates without any contribution to the other rock units. The strong increase of eU/eTh ratio with eU and not with eTh and K suggests post magmatic redistribution of uranium. This could be a favorable economic criterion for uranium mineralization, because uranium is likely to be remobilized and reconcentrated.

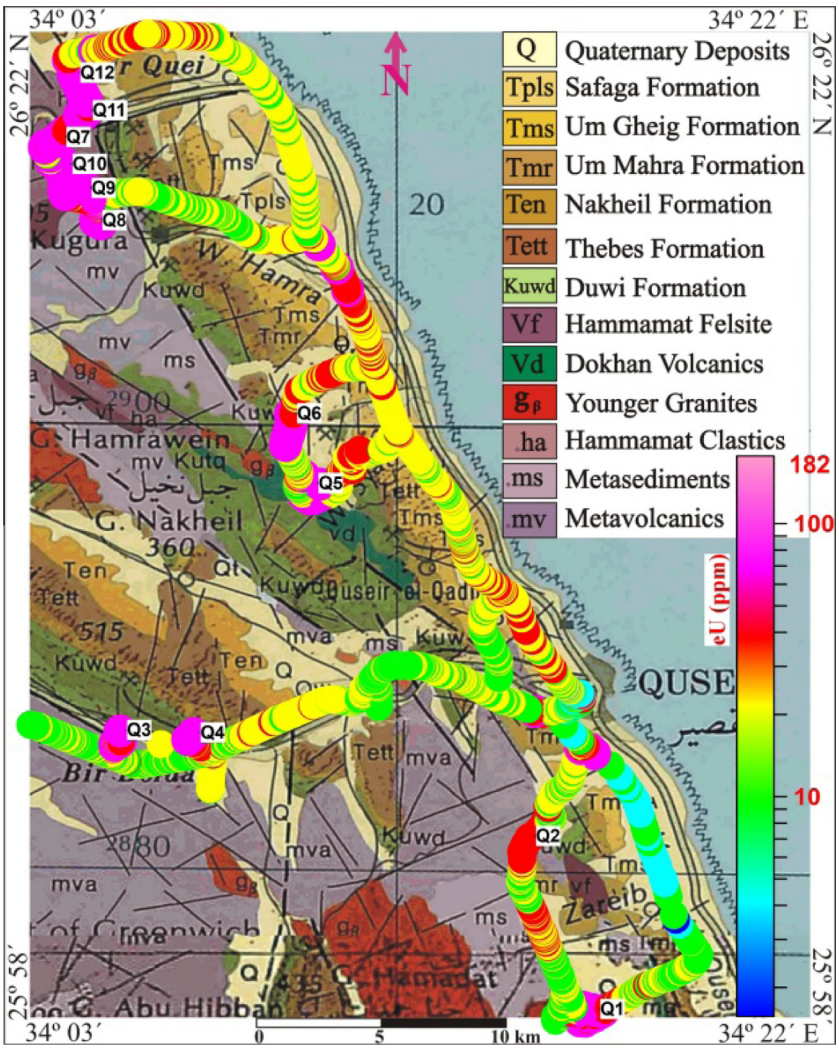

Figure 4 eU (ppm) image distribution map of Quseir-Safaga area, Central Eastern Desert, Egypt.

4. Results of X-ray analysis

This study deals with the estimation of 14 trace elements: (Cr, Cd, Co, Ni, Cu, Zn, Zr, Rb, Y, Ba, Pb, Sr, V and Nb) in the 12 phosphate samples using X-ray fluorescence technique. Some of them, such as phosphate, contain abundant trace elements (Bech et al., 2009). Determination of trace elements, present in environmental samples, is of considerable interest because of the increased awareness about environmental pollution and human health since some elements which are nutrients, can also act as toxin, if they are present above certain limits (Hayumbu et al., 1995). Phosphate ores of different geographical provenances can vary substantially in trace element contents. Therefore, in order to minimize environmental and health risks, it is important to know the phosphate trace element assemblages, and use suitable phosphates of known provenance with low potential toxic trace element contents.

The concentrations of trace elements in phosphate samples at Quseir-Safaga area were measured at NMA and are listed in Table 2. It is clear that the average concentrations (in ppm) of the trace elements for phosphate samples, in a decreasing order, are as follows: Sr (751) > Zn (297) > Cr (121) > Ba (99) > V (90) > Y (56) > Zr (15.1) > Ni (14.7) > Cu (13.4) > Pb (6.6). The average concentrations of trace elements in Quseir-Safaga samples are also shown in Table 2 and Fig. 7. It is clear that all samples contain high concentration of Strontium (Sr) and Zinc (Zn).

Table 2 shows the concentrations of Cr from 91 to 160 ppm, Ni from 5 to 27 ppm, Cu from 11 to 16 ppm, Zn from 47 to 1358 ppm, Zr from 9 to 24 ppm, Y from 40 to 121 ppm, Ba from 31 to 340 ppm, Pb from <2 to 24 ppm, Sr from 451 to 1047 ppm and V from 42 to 173 ppm. The lowest values of Ni, Cu, Zr and Ba are in sample No. Q12, Zr, Y, Pb and Sr are in Q7, Cr and Cu are in Q1 and V in Q3 and Q5. Meanwhile, the highest values of Cr, Ni and V are in sample Q8, Zr, Y, Ba and Sr in sample Q9, Cu in sample Q7, Zn in sample Q2 and Pb in sample Q1.

5. Gamma-ray spectroscopic analysis

Each phosphate sample was placed in a 500 g airtight PVC container. The inner lid was placed in and closed tightly with outer cap. The container was sealed hermetically and externally using cellophane tape and kept aside for about one

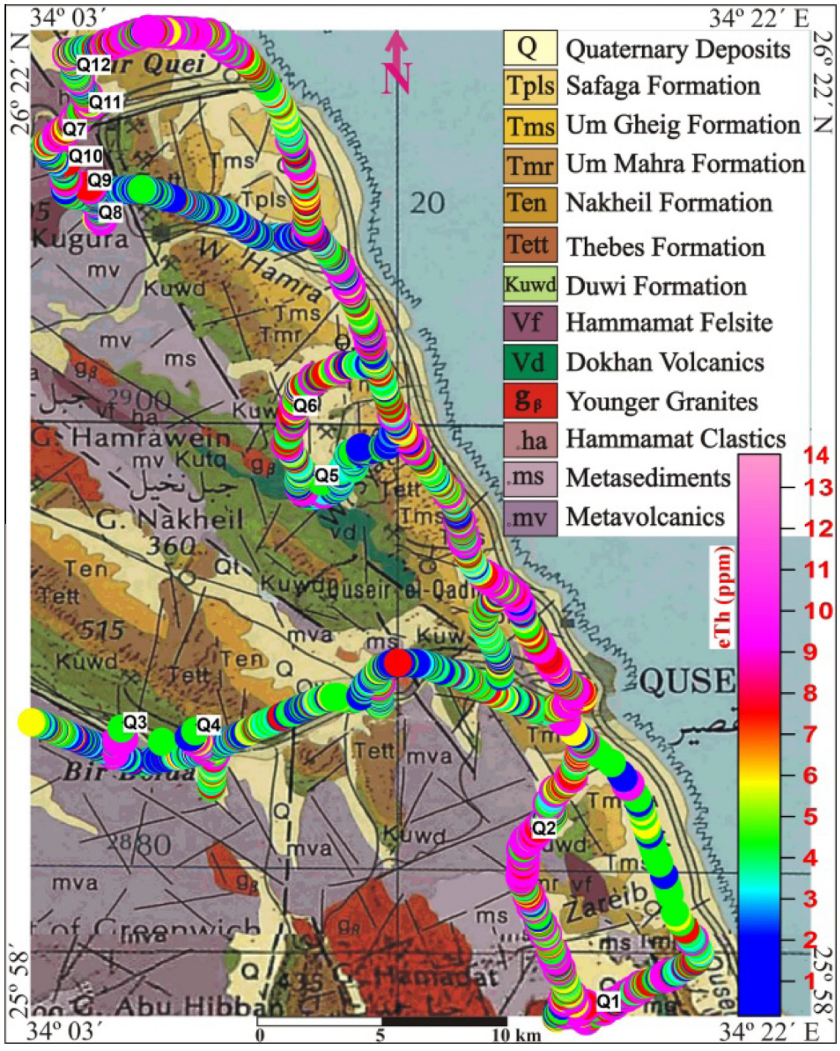

Figure 5 eTh (ppm) image distribution map of Quseir-Safaga area, Central Eastern Desert, Egypt.

month to ensure equilibrium between Ra and its daughter products, before being taken for gamma-ray spectrometric analysis.

To estimate the activity levels of ^{238}U, ^{232}Th and ^{40}K in the 12 samples, a high resolution gamma-ray detection system in the Laboratories of the Nuclear Physical Division, Faculty of Girls, Ain Shams University, was used for gamma-ray analysis. The detection system is basically a hyper pure germanium (HPGe), model No. GEM-15190, coaxial type detector with a serial No. 27-p-1876A recommended operating bias, negative 3 kV. The individual samples were placed on the detector manually during the work and each sample was analyzed for a time of 70,000 s. The γ-ray emitting radionuclides, specifically recorded, were as follows: ^{238}U, ^{232}Th, ^{226}Ra and ^{40}K.

Natural radionuclides of relevance for this work are mainly gamma-ray emitting nuclei in the decay series of ^{238}U and ^{232}Th, and single occurring ^{40}K. Meanwhile, ^{40}K can be measured directly by its own gamma-rays, ^{238}U and ^{232}Th are not directly gamma-ray emitters, but they are possibly measured by the gamma-ray of their decay products. Decay products for ^{238}U (^{214}Pb: 295 & 352 keV; and ^{214}Bi: 609 keV) and ^{232}Th (^{228}Ac: 209, 338 and 911 keV; ^{212}Pb: 239 keV; ^{212}Bi: 727 keV; and ^{208}TI: 583 keV) were used for the measurements of their parents, assuming the decay series to be in secular equilibrium (Firestone and Shirley, 1998). Weighted averages of several decay products were used to estimate activity concentrations of ^{238}U and ^{232}Th. The natural abundance of ^{235}U is only 0.72% of the total uranium content and hence was not considered in the present study.

5.1. Radiation health hazards

Radium equivalent activity (Ra_{eq}) is a widely used index in radiation health hazards. It can be obtained from the following equation (Ravisankar et al., 2012):

$$Ra_{eq} = A_{Ra} + 1.43A_{Th} + 0.077A_K \quad (1)$$

where A_{Ra}, A_{Th} and A_K are the activities of ^{226}Ra, ^{232}Th and ^{40}K, respectively, in Bq/kg. The maximum value of Ra_{eq} must be less than 370 Bq/kg, in order to keep the annual external absorbed dose safe and less than 1.0 mSv/y (UNSCEAR, 2000; USEPA, 2004).

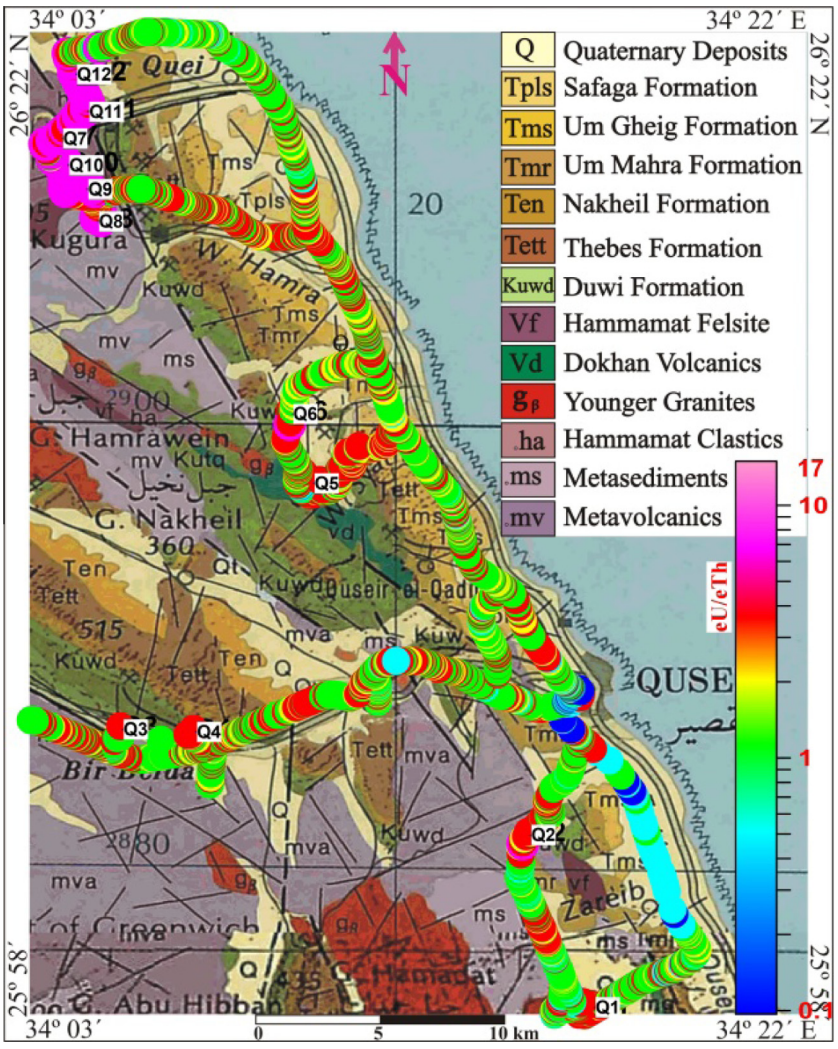

Figure 6 eU/eTh image distribution map of Quseir-Safaga area, Central Eastern Desert, Egypt.

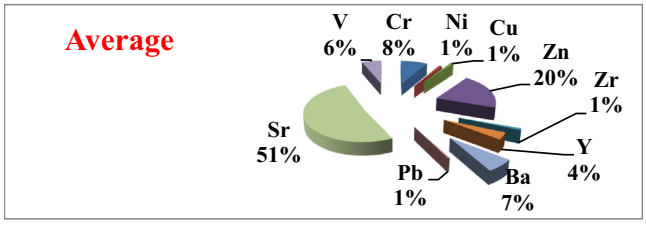

Figure 7 Average concentrations of trace elements (%) for phosphate samples of Quseir-Safaga area, Central, Eastern Desert, Egypt.

The absorbed dose rate due to γ-radiation in air at 1 m above the ground surface was also calculated. The conversion factors used for (D_R) calculations are 0.462 nGy/h for ^{226}Ra, 0.621 nGy/h for ^{232}Th, and 0.0417 nGy/h for ^{40}K. Accordingly, D_R can be calculated as follows (UNSCEAR, 2000):

$$D_R = 0.462A_{Ra} + 0.621A_{Th} + 0.0417A_K \quad (2)$$

where A_{Ra}, A_{Th} and A_K are the activities of ^{226}Ra, ^{232}Th and ^{40}K, respectively, in Bq/kg.

Table 1 The concentrations of the three radioelements and eU/eTh ratio for the 12 representative samples from the 12 phosphate mining of Quseir-Safaga area, Central Eastern Desert, Egypt.

Sample	Long. (E)	Lat. (N)	K (%)	eU (ppm)	eTh (ppm)	eU/eTh
Q1	34°17′02″	25°59′15″	0.5	66	7.7	8.6
Q2	34°16′20″	26°03′31″	0.2	35	3.2	10.9
Q3	34°06′45″	26°05′20″	0.3	57	3.7	15.4
Q4	34°07′40″	26°05′17″	0.3	98	5.4	18.1
Q5	34°10′52″	26°11′17″	0.3	80	4.8	16.7
Q6	34°10′33″	26°12′40″	0.6	77	8.6	9.0
Q7	34°06′11″	26°17′34″	0.8	97	9.1	10.7
Q8	34°06′12″	26°16′57″	0.3	143	7.3	19.6
Q9	34°05′58″	26°17′42″	0.3	182	9.7	18.8
Q10	34°05′33″	26°18′15″	0.3	152	8.3	18.3
Q11	34°05′59″	26°19′26″	0.2	116	7.8	14.9
Q12	34°05′43″	26°20′16″	0.3	85	6.1	13.9
Min	34°05′33″	25°59′15″	0.2	35	3.2	8.6
Max	34°17′02″	26°20′16″	0.8	182	9.7	19.6
Average	34°11′17″	26°10′30″	0.37	99	6.8	14.6

Table 2 Trace element contents (ppm) of phosphate samples at Quseir-Safaga area, Central Eastern Desert, Egypt.

Sample	Cr	Ni	Cu	Zn	Zr	Y	Ba	Pb	Sr	V
Q1	91	14	11	455	17	62	63	24	834	64
Q2	101	7	12	1358	11	43	130	12	602	68
Q3	154	7	15	71	13	46	36	2	696	42
Q4	109	18	15	131	18	62	79	3	972	110
Q5	134	21	14	369	13	46	36	2	696	42
Q6	116	18	12	103	16	57	113	6	798	117
Q7	153	9	16	120	9	40	92	<2	451	105
Q8	160	27	14	258	15	52	134	3	733	173
Q9	122	26	12	317	24	121	340	4	1047	157
Q10	103	14	14	202	14	51	81	11	773	86
Q11	119	10	15	129	18	46	50	3	686	62
Q12	93	5	11	47	13	44	31	3	719	48
Min	91	5	11	47	9	40	31	<2	451	42
Max	160	27	16	1358	24	121	340	24	1047	173
Average	121	14.7	13.4	297	15.1	56	99	6.6	751	90

Table 3 Activity concentration of radionuclides (in Bq/kg) of Quseir-Safaga 12 phosphate samples, Central Eastern Desert, Egypt.

Sample No.	^{238}U series (in Bq/kg)				^{232}Th series (in Bq/kg)			^{235}U (Bq/kg)
	^{234}Pa	^{226}Ra	^{214}Bi	^{214}Pb	^{228}AC	^{208}Tl	^{212}Pb	
Q1	946	1039	521	544	38.2	84.1	6.7	33.0
Q2	864	963	484	477	18.6	87.6	5.2	26.4
Q3	1339	1527	774	824	19.3	87.6	5.4	38.2
Q4	2193	2711	1272	1374	27.0	137.0	51.0	82.2
Q5	2565	2528	1451	1549	115	162	10.7	100.7
Q6	1205	1892	864	935	129.3	62.0	41.9	66.0
Q7	1226	1056	741	1620	20.8	57.7	6.8	57.7
Q8	2321	3265	1379	1542	43.0	69.4	7.2	101.7
Q9	2724	2875	1395	1505	51.0	62.3	2.0	80.7
Q10	3104	3309	1584	1671	57.5	85.1	4.6	91.0
Q11	1415	1742	872	874	43.4	98.5	29.6	54.2
Q12	1288	1928	883	967	198	116	6.2	59.1
Min	864	963	484	477	18.6	57.7	2	26.4
Max	3104	3309	1584	1671	198	162	51	101.7
Average	1766	2070	1018	1157	63	92	15	66

The annual effective dose (Eff. Dose) is a concept that allows the radiation doses from different radionuclides and from different types and sources of radioactivity to be added. The annual effective dose rate (in mSv/y) can be calculated using the following equation (UNSCEAR, 2000):

$$\text{Eff. Dose} = D_R \times 8760 \times 0.7 \times 0.2 \times 10^{-6} \quad (3)$$

where 0.7 Sv/Gy is the conversion coefficient from absorbed dose to effective dose and 0.2 is the fraction of time spent outdoors.

The external hazard index (H_{ex}) considers only the external exposure risk due to γ-rays and can be obtained by the following relation (Bereka and Mathew, 1985):

$$H_{ex} = A_{Ra}/370 + A_{Th}/259 + A_K/4810 \quad (4)$$

where A_{Ra}, A_{Th} and A_K are the activities of ^{226}Ra, ^{232}Th and ^{40}K, respectively, in Bq/kg.

The internal exposure to ^{222}Rn and its daughter products is controlled by an internal hazard index H_{in} which is defined as

$$H_{in} = A_{Ra}/185 + A_{Th}/259 + A_K/4810 \quad (5)$$

If the maximum concentration of radium is half that of the normal acceptable limit, then H_{in} will be $\leqslant 1$ (Abdullah, 2010).

The representative level index can be calculated using the following relation (Ebaid and Bakr, 2012):

$$I_\gamma = \frac{1}{150}A_{Ra} + \frac{1}{100}A_{Th} + \frac{1}{1500}A_K \quad (6)$$

where A_{Ra}, A_{Th} and A_K are the activities of ^{226}Ra, ^{232}Th and ^{40}K, respectively, in Bq/kg.

The mass exhalation rate E_{Rn} (Bq kg^{-1} s) of ^{222}Rn was determined through the following equation:

$$E_{Rn} = A_{Rn} \times A_{Ra} \times \lambda_{Rn} \quad (7)$$

where λ_{Rn} is the decay constant ^{222}Rn (2.1×10^{-6} per s) (Addo et al., 2013).

5.2. Results of natural radioactivity

The concentrations and distribution of radionuclides in the 12 studied samples from Quseir-Safaga area were determined

Table 4 Activity concentrations of ^{238}U, ^{235}U, ^{232}Th, ^{226}Ra and ^{40}K for the 12 Quseir-Safaga phosphate samples, Central Eastern Desert, Egypt.

Sample	^{235}U (Bq/kg)	^{226}Ra (Bq/kg)	^{238}U (Bq/kg)	^{232}Th (Bq/kg)	^{40}K (Bq/kg)
Q1	33.0	1039	946	43.0	122
Q2	26.4	963	864	37.1	169
Q3	38.2	1527	1339	37.5	107
Q4	82.2	2711	2193	71.8	124
Q5	101	2528	2565	96.0	117
Q6	66.0	1892	1205	77.7	110
Q7	57.7	1056	1226	28.4	118
Q8	102	3265	2321	39.8	129
Q9	80.7	2875	2724	38.4	109
Q10	91.0	3309	3104	49.1	98
Q11	54.2	1742	1415	57.2	105
Q12	59.1	1928	1288	106	91
Min.	26	963	864	28.4	91
Max.	102	3309	3104	106	169
Average	66	2070	1766	57	117
W.A.	33	32	33	45	412

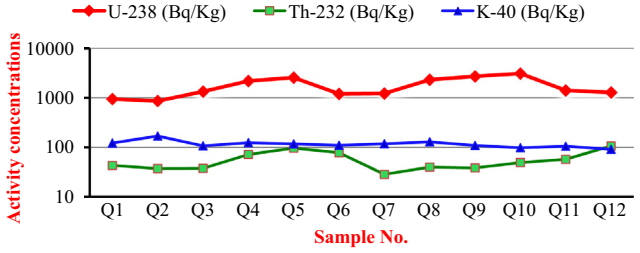

Figure 8 Activity concentrations in (Bq/kg) of ^{238}U, ^{232}Th and ^{40}K for Quseir-Safaga phosphate samples, Central Eastern Desert, Egypt.

using HPGe spectrometer to evaluate their environmental radioactivity.

The activity concentrations of ^{238}U were measured from ^{234}Pa (1001 keV), ^{226}Ra from (186 keV), ^{214}Pb from (352, 295 keV) and ^{214}Bi from (609, 1120, 1765 keV); meanwhile, the activity concentration of ^{228}Ac was measured from 911, 338.4 keV and Tl from 583, 2614 keV. They were used to evaluate the specific activity of ^{232}Th series radionuclides. ^{40}K was determined from 1460 keV photo peak. For the actinium series ^{235}U γ-energies of 144 keV and 163 keV were taken to represent the ^{235}U activity (Merdanoglu and Altinsoy, 2006).

Table 3 shows the activity concentrations of the radionuclides of the 12 Quseir-Safaga phosphate samples. The radionuclides of ^{238}U series are ^{234}Pa, ^{226}Ra, ^{214}Bi and ^{214}Pb while for ^{232}Th series are ^{228}Ac, ^{208}Tl and ^{212}Pb. The activity concentrations of ^{238}U series are included in ^{234}Pa that varies from 864 to 3104 Bq/kg, ^{226}Ra varies from 963 to 3309 Bq/kg, ^{214}Bi from 484 to 1584 Bq/kg, and ^{214}Pb from 477 to 1671 Bq/kg. Meanwhile, ^{232}Th series has values of ^{228}Ac that ranges from 19 to 198 Bq/kg, ^{208}Tl from 58 to 162 Bq/kg, and ^{212}Pb from 2.04 to 51 Bq/kg. ^{235}U was found to vary from 26 to 102 Bq/kg.

The activity concentrations of ^{238}U range from 864 to 3104 Bq/kg, ^{232}Th from 28.4 to 106 Bq/kg, ^{226}Ra from 963 to 3309 Bq/kg, ^{40}K from 91 to 169 Bq/kg and ^{235}U from 26 to 102 Bq/kg (Table 4 and Fig. 8).

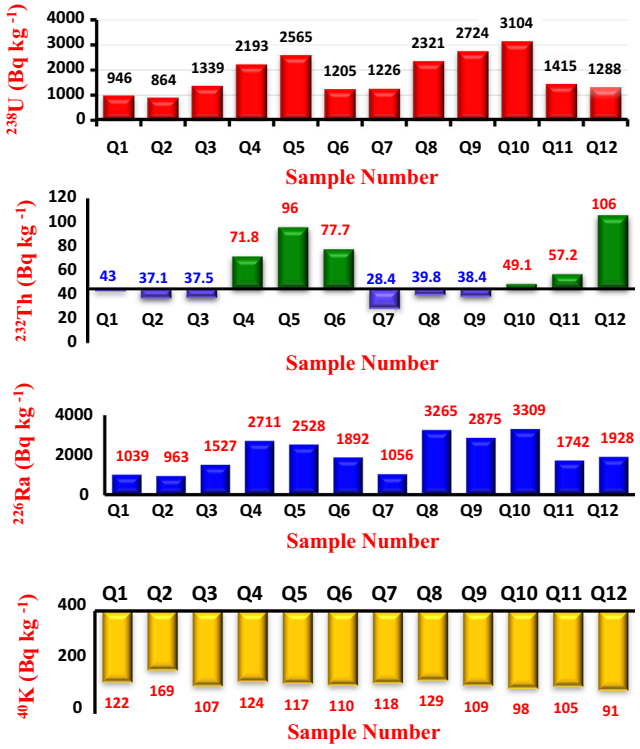

Figure 9 Activity concentration of ^{238}U, ^{232}Th, ^{226}Ra and ^{40}K (in Bq kg^{-1}), Quseir-Safaga phosphate samples, Central Eastern Desert, Egypt.

The radioelements worldwide average (W.A.) values are 33 Bq/kg for ^{238}U, 32 Bq/kg for ^{226}Ra, 45 Bq/kg for ^{232}Th and 412 Bq/kg for ^{40}K (UNSCEAR, 2008). The data on worldwide average outdoor dose rates value is 58 nGy/h (UNSCEAR, 2008). The concentrations of all Quseir-Safaga phosphate samples are higher than the worldwide average (33 and 32 Bq/kg) for ^{238}U and ^{226}Ra respectively (Table 4 and Fig. 9). Meanwhile, the concentrations of six phosphate

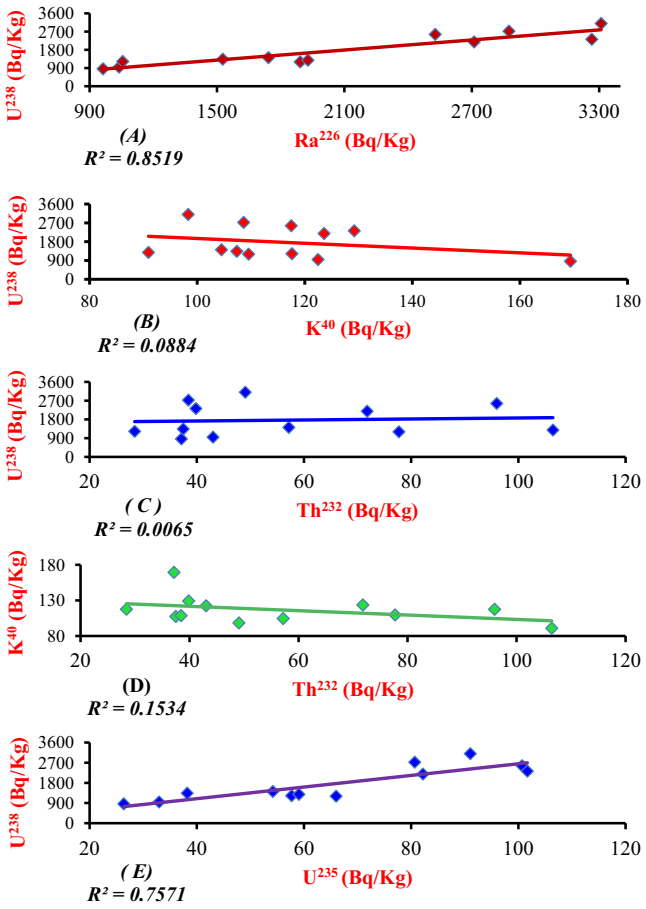

Figure 10 Correlation of the activity concentrations between A – (^{238}U & ^{226}Ra), B – (^{238}U & ^{40}K), C – (^{238}U & ^{232}Th), D – (^{40}K & ^{232}Th) and E – (^{238}U & ^{235}U) in Quseir-Safaga phosphate samples, Central Eastern Desert, Egypt.

samples are lower than the worldwide average (W.A.) of 45 Bq/kg for thorium while the samples (Q4, Q5, Q6, Q10, Q11 and Q12) have concentrations higher than the worldwide average. On the other hand, the concentrations of all Quseir-Safaga phosphate samples are lower than the worldwide level for potassium (412 Bq/kg) (Table 4 and Fig. 9).

Correlations between ^{238}U and ^{226}Ra, ^{238}U and ^{40}K, ^{232}Th and ^{40}K, ^{238}U and ^{235}U are displayed in Fig. 10A–E. The resultant correlations are weak in Fig. 10B–D and strong in Fig. 10A and E. There is a high and positive correlation between ^{238}U and ^{226}Ra (R^2 = 0.8519) and also a high and positive correlation between ^{238}U and ^{235}U (R^2 = 0.7571) because the two elements accompany each other. Meanwhile, Fig. 10B shows a negative correlation between ^{238}U and ^{40}K (R^2 = 0.0884), which could be indication of high U-enrichment. Fig. 10C shows weak correlation between ^{238}U and ^{232}Th (R^2 = 0.0065) due to the lower activity concentration of ^{232}Th compared with the high re-concentrated ^{238}U. Fig. 10D shows a poor negative correlation between ^{232}Th and ^{40}K (R^2 = 0.1534), which indicates moderate activity concentration level of ^{232}Th compared to very low ^{40}K activity concentration.

The specific activity of a sample containing 1.0 ppm, by weight, of ^{238}U is 12.35 Bq/kg, 1.0 ppm of Ra is 11.1 Bq/kg, 1 ppm of ^{232}Th is 4.06 Bq/kg and 1% of ^{40}K is 313 Bq/kg, (El Galy et al., 2008). For ^{235}U the specific activity concentration also given in ppm is considered as 1 ppm = 80 Bq/kg (Barton, 1995).

The radionuclide concentration of ^{238}U series, ^{232}Th series and ^{40}K varies between 70 and 251 ppm, 7 and 26.2 ppm and 0.29% and 0.54% respectively (Table 5). The arithmetic mean of all studied phosphate samples (0.11) of ^{232}Th/^{238}U ratio is much lower than the Clark's value (3.5), which indicates U-enrichment in the phosphates in the studied area. ^{238}U/^{226}Ra ratios for most of the 12 phosphate samples are lower than unity, reflecting a state of radioactive disequilib-

Table 5 Concentrations of ^{238}U, ^{232}Th, ^{40}K and (^{232}Th/^{238}U) ratio for Quseir-Safaga phosphate samples, Central Eastern Desert, Egypt.

Samples	^{238}U (ppm)	^{232}Th (ppm)	^{235}Un (ppm)	^{226}Ra (ppm)	^{40}K (%)	^{238}U /^{226}Ra	^{232}Th/^{238}U
Q1	77	10.6	0.41	94	0.39	0.82	0.14
Q2	70	9.2	0.33	87	0.54	0.80	0.13
Q3	108	9.2	0.48	138	0.34	0.78	0.09
Q4	178	17.7	1.03	244	0.40	0.73	0.10
Q5	208	23.6	1.26	228	0.38	0.91	0.11
Q6	98	19.1	0.83	170	0.35	0.58	0.19
Q7	99	7.0	0.72	95	0.38	1.04	0.07
Q8	188	9.8	1.27	294	0.41	0.64	0.05
Q9	221	9.5	1.01	259	0.35	0.85	0.04
Q10	251	12.1	1.14	298	0.31	0.84	0.05
Q11	115	14.1	0.68	157	0.33	0.73	0.12
Q12	104	26.2	0.74	174	0.29	0.60	0.25
Min	70	7.0	0.33	87	0.29	0.80	0.04
Max	251	26.2	1.27	298	0.54	0.84	0.25
Average	143	14.0	0.83	186	0.37	0.77	0.11

Table 6 Values of radium equivalent (Ra_{eq}), external hazard (H_{ex}), internal hazard (H_{in}), external gamma radiation (I_γ), dose rate (D_R) and the effective dose (Eff. Dose) for Quseir-Safaga phosphate samples, Central Eastern Desert, Egypt.

Samples	Ra_{eq} (Bq/kg)	H_{ex} (nGy/y)	H_{in} (nGy/y)	I_γ	D_R (nGy/h)	Eff. Dose (mSv/y)
Q1	1110	3.0	5.8	7.5	468	0.57
Q2	1030	2.8	5.4	6.9	429	0.53
Q3	1589	4.3	8.4	10.7	646	0.79
Q4	2823	7.6	15.0	19.0	1062	1.30
Q5	2674	7.2	14.1	18.0	1248	1.53
Q6	2011	5.4	10.6	13.5	608	0.75
Q7	1105	3.0	5.8	7.4	588	0.72
Q8	3332	9.0	17.8	22.4	1102	1.35
Q9	2938	7.9	15.7	19.7	1286	1.58
Q10	3387	9.2	18.1	22.7	1468	1.80
Q11	1832	5.0	9.7	12.3	692	0.85
Q12	2088	5.6	10.9	14.1	663	0.81
Min	1030	2.8	5.4	6.9	429	0.53
Max	3387	9.2	18.1	22.7	1468	1.8
Average	2160	5.8	11.4	14.5	855	1.05
P.L.	370	1.0	1.0	1.0	58	1.0

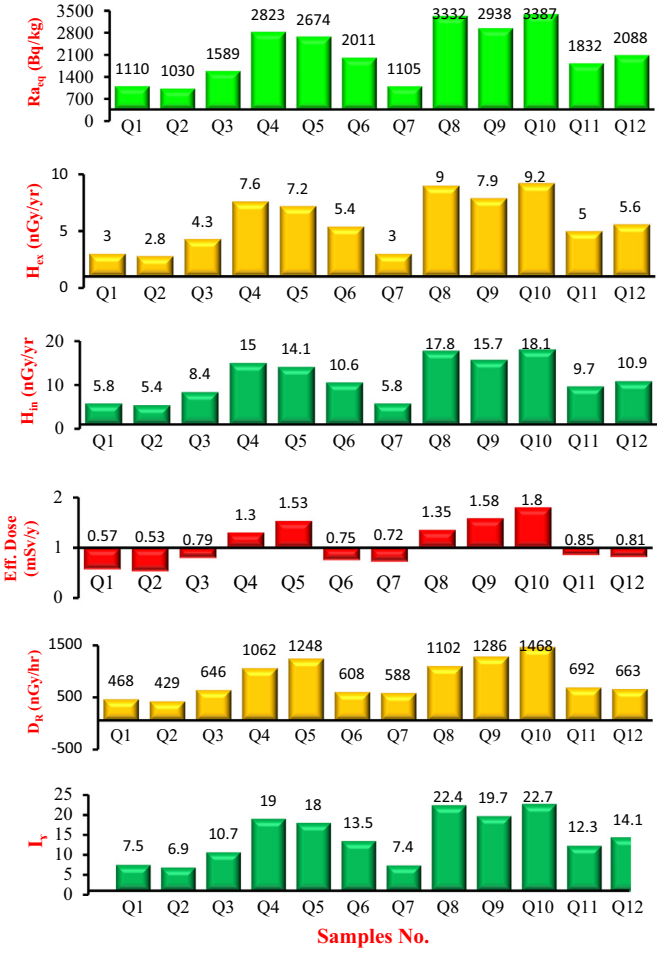

Figure 11 Values of radium equivalent (Ra_{eq}) in (Bq/kg), external and internal hazard (H_{ex} & H_{in}) in (mGy/y), external gamma radiation (I_γ), dose rate (D_R) in (nGy/h) and effective dose (Eff. Dose) in (mSv/y) for Quseir-Safaga phosphate samples, Central Eastern Desert, Egypt.

Table 7 Values of activity of ^{226}Ra (A_{Ra}), emanation coefficient of radon (C_{Rn}), emanation factor (F) and mass exhalation rate of radon (E_{Rn}) for Quseir-Safaga 12 phosphate samples, Central Eastern Desert, Egypt.

Sample No.	A_{Ra} (Bq/kg)	C_{Rn} (Bq/kg)	F	E_{Rn} (μBq/kg)
Q1	1039	518	0.50	1.1
Q2	963	479	0.50	1.0
Q3	1527	753	0.49	2.4
Q4	2711	1439	0.53	8.2
Q5	2528	1076	0.43	5.7
Q6	1892	1028	0.54	4.1
Q7	1056	315	0.30	0.7
Q8	3265	1886	0.58	12.9
Q9	2875	1480	0.52	8.9
Q10	3309	1725	0.52	12.0
Q11	1742	870	0.50	3.2
Q12	1928	1045	0.54	4.2
Min	963	315	0.30	0.7
Max	3309	1886	0.58	12.9
Average	2070	1051	0.50	5.4

rium between U and its daughter, ^{226}Ra (Table 5). This state of disequilibrium is mostly related to high U-enrichment.

The radium equivalent (Ra_{eq}) ranges from 1030 to 3387 Bq kg^{-1} which is higher than the recommended value 370 Bq kg^{-1} (Table 6). A modified quantity of radium equivalent activity is the external and internal hazard indices. These indices must be lower than unity in order to keep the radiation hazard insignificant (UNSCEAR, 2000). The calculated values of the external hazard range from 2.8 to 9.2 nGy/y whereas, those of the internal hazard range from 5.4 to 18.1 nGy/y (Table 6). The values of radioactivity level index I_γ are mostly more than unity, which vary between 6.9 and 22.7 Bq kg^{-1} (Table 6 and Fig. 11). The dose rates range from 429 to 1468 nGy/h, with a mean reaching 855 nGy/h, which is largely higher than the international mean value of 58 nGy/h (UNSCEAR, 2008).

5.2.1. The activity concentration of U-238 was measured from Pa-234m (1001 keV)

The effective doses range from 0.53 to 1.8 mSv/y, with a mean reaching 1.05 mSv/y. Five samples (Q4, Q5, Q8, Q9 and Q10) have effective dose values more than the permissible level (P. L.) of unity (Table 6 and Fig. 11).

The values of activity of ^{226}Ra (A_{Ra}), emanation coefficient of radon (C_{Rn}), Emanation factor (F) and mass exhalation rate of radon (E_{Rn}) are shown in Table 7. The values of activity of ^{226}Ra (A_{Ra}) range from 963 to 3309 Bq/kg. The emanation coefficient of radon (C_{Rn}) ranges from 315 to 1886 (Bq/kg). The emanation factor (F) ranges from 0.3 to 0.58. The mass exhalation rate of radon (E_{Rn}) ranges from 0.7 to 12.3 (μBq/kg).

Fig. 12 shows a strong correlation between radon mass exhalation rate (E_{Rn}) and activity of ^{226}Ra (A_{Ra}) with correlation coefficient $R^2 = 0.9513$, which means that E_{Rn} and A_{Ra} accompany with each other.

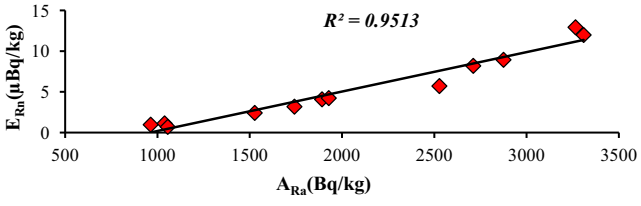

Figure 12 Correlation between radon mass exhalation rate (E_{Rn}) and activity of ^{226}Ra (A_{Ra}) for Quseir-Safaga phosphate samples, Central Eastern Desert, Egypt.

6. Conclusions

High-sensitivity carborne γ-ray spectrometric survey proves high concentrations of eU ranging from 34 ppm to 182 ppm associated with locations of phosphate mines which are considered high risk for populations. The northwestern part of the study area possesses the highest content of eU. Meanwhile, all phosphate mines represent the lowest level of both eTh and K concentrations in the study area. The remaining rock types of the study area, which include older granites, metavolcanics and ophiolites as well as sedimentary rocks, are saved where they are free from any high radioelements concentrations.

The concentrations of trace elements in phosphate samples at Quseir-Safaga area reveal high concentration of both Strontium (Sr) and Zinc (Zn) with an average 51% and 20% respectively.

The current study estimated the activity concentrations of the three radionuclides: ^{226}Ra, ^{238}U, ^{232}Th and ^{40}K by means of gamma-ray spectrometry in twelve phosphate samples in Quseir-Safaga area, Central Eastern Desert, Egypt. The average values of activity concentrations of ^{226}Ra, ^{238}U, ^{232}Th and ^{40}K in these 12 samples were 2070 Bq/kg, 1766 Bq/kg, 57 Bq/kg and 117 Bq/kg respectively. The maximum concentrations of ^{226}Ra, ^{238}U, ^{228}Th and ^{40}K reached 3309 Bq/kg, 3104 Bq/kg, 106 Bq/kg and 169 Bq/kg respectively. Though, the area of large concentration of ^{238}U coincides with slightly high values of ^{232}Th but does not coincide with any high values of ^{40}K. The total annual effective doses which could be received by members of the public from exposition to phosphate mines ranged from 0.53 mSv/y to 1.8 mSv/y, with an average value of 1.05 mSv/y, which is higher than the worldwide value of 1.0 mSv/y for the permitted public exposure.

References

Abdullah, A., 2010. The effect of grain size on the measurements of activity concentration of naturally occurring radioactive materials. Department of Phy., Faculty of Engineering and Physical Sciences, University of Surrey (MPhil to PhM Transfer Report).

Addo, A., Darko, O., Gordon, C., Nyarko, J.B., 2013. Evaluation of radiological hazard parameters in building materials used in a rural area of Ghana. Schol. Res. Lib. Arch. Phys. Res. 4 (3), 42–50.

Aissa, M., Jubeli, Y.M., 1997. Carborne gamma-ray spectrometric survey of an area east of Homs, Central Syria. Appl. Radiat. Isot. 48, 135–142.

Awad, G.H., Ghobrial, M.G., 1966. Zonal stratigraphy of Kharga Oasis. Ann. Geol. Surv. Egypt 34, 1–77.

Barton, J.C., 1995. Studied with a low-background germanium detector in the Holborn underground laboratory. Nucl. Instrum. Methods Phys. Res. 354, 530–538.

Bech, J., Suarez, M., Reverter, F., Tume, P., Sánchez, P., Lansac, A., 2009. Selenium and other trace elements in phosphate rock of Bayovar–Sechura (Peru). J. Geochem. Explor. 107 (2), 136–145.

Bereka, J., Mathew, P.J., 1985. Natural radioactivity of Australian building materials, industrial wastes and by-products. Health Phys. 48, 87–95.

Compton, J.S., 1997. Origin and paleoceanographic significance of Florida's phosphate deposits. The Geology of Florida. Univ. Press of Florida, Gainesville, USA, pp. 195–216.

Continental Oil Company (CONOCO), 1987. In: Klitzsch, List, Phohlmann, Handley, Hermina, Meissner (Eds.), Geological Map of Egypt, Scale 1:500,000, Cairo.

Dabous, A.A., 1981. Mineralogy, geochemistry, and radioactivity of some Egyptian phosphate deposits, Ph.D. Thesis, Florida State Univ., Tallahassee, Florida, USA, 202 p.

Ebaid, Y.Y., Bakr, W.F., 2012. Investigating the effect of using granite and marble as a building material on the radiation exposure of humans. Radiat. Prot. Dosimetry. http://dx.doi.org/10.1093/rpd/ncs044, pp. 1–8.

El Galy, M.M., El Mezayen, A.M., Said, A.F., El Mowafy, A.A., Mohamed, M.S., 2008. Distribution and environmental impacts of some radionuclides in sedimentary rocks at Wadi Naseif area, Southwest Sinai, Egypt. Environ. Rad. 99, 1075–1082.

Firestone, R.D., Shirley, V.S., 1998. Table of Isotopes, eighth ed. John Wiley, New York.

Gaafar, I.M., Abu Halawa, A., Sroor, A., Elbarbary, M., 2012. Environmental Assessment for Natural Radioactivity of El Arish Beach Sands, Northern Coast of Sinai, Egypt. J. Environ. Sci. 40 (3), 277–296.

Gaafar, I.M., Ali, K.G., Meira, M.I., 2014. Integration of airborne and carborne gamma-ray spectrometric surveys, Wadi Elgidami area, Central Eastern Desert, Egypt. Egypt. Geophys. Soc. J. 12, 65–78.

Gaafar, I.M., Aboelkheir, H., Bayoumi, M., 2016. Integration of gamma-ray spectrometric and aster data for uranium exploration in Qash Amer-El-Sela area, Southeastern Desert, Egypt. Nucl. Sci. Sci. J. 5, 51–69.

Grasty, R.L., Cox, J.R., 1997. A carborne gamma-ray spectrometer system for natural radioactivity mapping and environmental monitoring. Rapid Environ. Survey. Mob. Equip. NKS, ISBN: 87-7893-014-6.

Hayumbu, P., Zaman, M.B., Lubaba, N.C.H., Munsanje, S.S., Muleya, D., 1995. Natural radioactivity in Zambian building materials collected from Lusaka. J. Radio Anal. Nucl. Chem. Lett. 11, 299.

IAEA, 2010. Radioelement mapping. IAEA Nuclear Energy Series, No. nf-t-1.3. International Atomic Energy Agency, Vienna, 123 p.

James, B.N., Dileep, R.M., Mulla, R.M., Joshi, M.S., Vishnu, P.D., Nayak, P.M., Sarkar, P.K., 2013. Evaluation of international dose to members of the public at the Kaiga site, India. Radiat. Prot. Dosimetry 153, 56–63.

Karlsson, S., Mellander, H., Lindgren, J., Finck, R., Lauritzen, B., 2000. Rapid environmental surveying using mobile equipment. NKS-15, ISBN: 87-7893-065-0.

Khoury, H.N., Al-Hawari, Z.Q., El-Suradi, S., 1988. Clay minerals associated with Jordanian phosphates and their possible industrial utilization. Appl. Clay Sci. 3, 111–121.

Merdanoglu, B., Altinsoy, N., 2006. Radioactivity concentration and dose assessment for soil samples from kestanbole granite area, Turkey. Radiat. Prot. Dosimetry. 121 (4), 399–405.

Notholt, A.J.G., 1985. Phosphate resources in the Mediterranean Tethyan phosphogenic province: a progress report. Sci. Geolog. Memoir 77, 9–21.

Paschoa, A.S., Godoy, J.M., 2002. The high natural radioactivity and TENORM wastes. In: International Congress Series I225. High Levels of Natural Radiation and Radon Areas. Elsevier Science, Amsterdam, pp. 3–8.

Prevot, L., 1990. Geochemistry, petrography, genesis of Cretaceous-Eocene phosphates: the Ganntour deposit (Morocco) – a type example. Soc. Geol. France, Memoire, No. 158, 232 p.

Raghuwanshi, S.S., 1992. Airborne gamma-ray spectrometry in uranium exploration. Adv. Space Res. 12, 77–86.

Ravisankar, R., Vanasundari, K., Chandra sekaran, A.M., Suganya, P., Vijayagopal, V., 2012. Measurement of Natural radioactivity in building materials of Namakkal, Tamilnadu, India using gamma ray spectrometry. Appl. Radiat. Isotop. 70, 699–704.

Sanderson, D.W., Cresswell, A.J., Lang, J.J., 2003. An International Comparison of Airborne and Ground based Gamma Ray Spectrometry. University of Glasgow, Scotland, UK, ISBN 08-5261-783-6.

Shanthi, G., Kumaran, T., Raj, A.G., Maniyan, C.G., 2010. Natural radionuclides in the South Indian foods and their annual dose. Nucl. Instrum. Methods Phys. Res. 619, 436–440.

Sharafeldin, A.A., 1999. Some geological aspects of the Egyptian phosphates. Ph.D. Thesis, Ain-Shams Univ., Cairo, Egypt, 294 p.

Tauchid, M., Jubeli, Y., 1991. Uranium exploration in Syria. SYR/86/005, Terminal Report, IAEA, Vienna, Austria.

Ulvsand, T., Finck, R.R., Lauritzen, B., 2002. Barents Rescue 2001 LIVEX. NKS-54, ISBN: 87-7893-108-8.

UNSCEAR, 2000. Sources and effects of ionizing radiation. United Nations Scientific Committee on the Effects of Atomic Radiation Sources to the General Assembly with Annexes, Effects and Risks of Ionizing Radiation, United Nations Publications, New York.

UNSCEAR, 2008. Sources and effects of ionizing radiation, V. I: Sources. Report to the General Assembly, Scientific Annexes A and B. United Nations Scientific Committee on the Effects of Atomic Radiation. United Nations Sales Publication E. 10. XI. 3. United Nations, New York.

United States Environmental Protection Agency (USEPA), 2004. A Citizen's Guide to Radon. The guide to protecting yourself and your family from Radon 402-k-02-006.

Vandenhove, H., 2000. European sites contaminated by residues from the ore extracting and processing industries. In: Proceedings Series, STI/PUB/1092, IAEA, Vienna, pp. 61–89.